Structure and Properties of Polyurethane–Silica Nanocomposites

ZORAN S. PETROVIĆ,[1] IVAN JAVNI,[1] ALAN WADDON,[2] GYÖRGY BÁNHEGYI[3]

[1] Pittsburg State University, Kansas Polymer Research Center, 1501 S. Joplin, Pittsburg, Kansas 66762

[2] University of Massachusetts, Department of Polymer Science and Engineering, Amherst, Massachusetts 01003

[3] Furukawa Electric Institute of Technology, Budapest, Hungary

Received 11 May 1999; accepted 23 May 1999

ABSTRACT: Nanocomposites with different concentrations of nanofiller were prepared by adding nanosilica filler to the single-phase polyurethane matrix. A control series was prepared with the same concentrations of micron-size silica. The nanosilica filler was amorphous, giving composites with the polyurethane that were transparent at all concentrations. The nanocomposites displayed higher strength and elongation at break but lower density, modulus, and hardness than the corresponding micron-size silica-filled polyurethanes. Although the nanosilica showed a stronger interaction with the matrix, there were no dramatic differences in the dielectric behavior between the two series of composites. © 2000 John Wiley & Sons, Inc. J Appl Polym Sci 76: 133–151, 2000

Key words: polyurethane; nanosilica; composites; mechanical, electrical properties

INTRODUCTION

Fillers have important roles in modifying the properties of various polymers. The effect of fillers on properties of the composite depends on their concentration and their particle size and shape. as well as on the interaction with the matrix. The theory of filler reinforcement of polymers predicts the formation of a boundary layer of a matrix material on the surface of the filler.[1,2] The thickness of the layer depends on the strength of the interaction, with a stronger interaction producing a greater thickness. The properties of a polymer in the boundary layer differ from those in the bulk of the matrix material primarily due to the decreased mobility of adsorbed chains on the filler surface, resulting in a higher glass transition. If the particles are closely spaced, the total mass of the matrix material may be located in the boundary layers, thus giving the matrix entirely different properties than are usual. Also, fillers with a particle size in the nanometer range have a small number of atoms per particle and for this reason may have different properties than the bulk material. Additionally they have an extremely large surface-to-volume ratio and may have considerably stronger interactions with the matrix. The interparticle distance in filled materials is, of course, also a function of particle diameter and concentration. For example, for filler particles arranged on a cubic lattice, simple calculation shows the interparticle distance (surface to surface) to be about two diameters at 5% volume concentration, or one diameter at 10 vol %. For illustration, particles in a matrix with 10 vol % of a filler with 1-mm particle diameter will be separated by 1 mm, while particles of 1 nm will be 1 nm apart. In the second case the particles will "feel" each other if there is a strong interaction between the matrix and the filler (e.g., the bound-

Correspondence to: Z. S. Petrović (zpetrovi@pittstate.edu).

Journal of Applied Polymer Science, Vol. 76, 133–151 (2000)

ary layer thickness in polyurethane; hard domains in the soft-phase matrix was estimated to be about 0.8 nm).[3] Under such circumstances the separation of filler particles is on the order of molecular dimensions, which may also have consequences for the matrix behavior. The above illustrates the opportunities for using nanofillers for modification of properties of polymeric matrices.

A second important factor stems from the nanoparticles themselves possibly exhibiting properties different from those in larger particles, for example in the areas of optical, electrical, and magnetic properties. Since nanoparticles are much smaller than the wavelength of visible light, the composites may be transparent, although the same matrix with larger particles may not.

The effect of the concentration of 12-nm silica particles on the properties of single-phase polyurethanes was investigated. In this case the single-phase polyurethanes were crosslinked rubbers consisting of polyols and diisocyanates. Such systems have considerably lower strength than two-phase segmented thermoplastic urethanes. The much higher strength of the latter are attributed to the existence of hard domains that act as crack propagation stoppers.[4] Since hard domains in soft elastomers are globules, typically around 10–20 nm in diameter,[5] the objective was set of testing the effect of fillers of a size comparable to that of hard domains on the properties of a single-phase urethane. The difference between silica- and hard-domain-filled polyurethanes is their morphology; the former does not change with increased filler concentration, while the domains of the latter become elongated to form rods or lamellae or become the continuous phase at high concentrations.[6] Thus, nanosilica-filled systems may serve as model systems for testing the effect of concentration on properties without changing morphology.

The effect of fillers on properties of elastomers is somewhat different from that its effect on glassy polymers. In reactive systems the particulate filler may have very different effects on the properties of the composite depending upon how it affects the curing process. If the particles react with the matrix, they may form firm bonds and improve strength, but they may also affect stoichiometry and cause incomplete curing. If the filler has a negative catalytic effect on curing, the matrix around particles will have a lower degree of curing and thus lower properties. Several authors have studied the effect of nanofillers generated *in situ* in silicone elastomers,[7–12] but few studies have been devoted to polyurethane nanocomposite elastomers.[13] Mark presented a review of the preparation and properties by the sol–gel route to organic–inorganic composites.[14] In this study we have avoided *in situ*–generated silica. Instead, we have used a well-defined, perfectly round, narrow size distribution (10–20 nm) of silica having an average diameter of 12 nm, dispersed in methyl ethyl ketone (MEK). Since spatial confinement in small particles affects a given property, when the size of the atomic ensemble becomes comparable to or smaller than the critical-length scale for the mechanism that is responsible for that property,[15] such changes can be expected. Since the metallic radius of silicon is 0.138 nm, fewer than 40 atoms can be placed along the diameter of the particle, discounting the volume taken by the oxygen atoms. Such changes should be reflected not only in the density and hardness, but also in the mechanical and dielectric properties. In order to analyze the effect of particle size, a series of composites filled with micron-size crystalline quartz was prepared. The filler concentration in poly(propylene oxide)/diphenylmethane diisocyanate (MDI) polyurethane networks in both series was varied from 0% to 50 wt %. The structure of the composites was studied by scanning electron microscopy (SEM), wide-angle X-ray diffraction (WAXD), and small-angle X-ray scattering (SAXS), Fourier transform infrared spectroscopy (FTIR) and UV/VIS spectroscopy. Physical, thermal, mechanical, and dielectric properties of composites were measured as a function of filler concentration.

EXPERIMENTAL

Materials

The polyurethane matrix was prepared from Multranol 3600 [poly(propylene oxide) diol from Bayer, MW = 2,000] and Multranol 3400 (PPO triol from Bayer, MW = 3,000), and crude diphenylmethane diisocyanate (MDI) from Mondur E-448 (Bayer, Pittsburgh, PA).

Nanosilica, MEK–ST, with an average particle diameter of about 12 nm, was obtained from Nissan Chemical Co. as a 30% dispersion in methyl ethyl ketone. The distribution of sizes was such that diameters lay between 10 and 20 nm. Crystalline quartz (microsilica) Min-U-Sil 5 (average

particle size 1.4 μm) was kindly supplied by U.S. Silica Co., Berkeley Springs, WV.

Methods

Polyurethane–filler composites were prepared by mixing polyol with the filler and removing MEK by distillation, with subsequent curing using diisocyanate at 100°C for 16 h in the presence of the 0.1% catalyst Cocure 55 (from CasChem). The weight ratio of diol to triol was 4:1 (molar ratio = 6:1). An excess of 5% of isocyanate was used to compensate for an unspecified amount of hydroxyl groups on the surface of the nanosilica. The mixture was then poured into a mold to obtain 1- and 2-mm thick sheets. The filler concentration was varied from 0% to 50% in steps of 10. The sample with 50% filler was tacky, probably due to the incomplete urethane reaction and the reaction of isocyanate with hydroxyl groups on the surface of silica or else to the adsorption of polyol chains on the filler surface. Poly(propylene oxide) polyols have a strong interaction with the nanosilica, which is manifested in a greater viscosity increase than in microsilica of the same concentration. The polyol gelled at 50% nanosilica but would flow if temperature were raised to 100°C. Such strong adsorption may have affected the curing process and contributed to the incomplete curing of the sample with 50% nanosilica.

A parallel series was prepared with microsilica, which for clarity will be called "microcomposites." WAXD, SAXS, and SEM were used to examine the structure of composites. WAXD was performed with a Siemens D500 diffractometer in transmission mode, using Ni-filtered CuKα radiation from a sealed tube generator. SAXS measurements were carried out using a pinhole collimated Rigaku-Denki camera with Ni-filtered CuKα radiation from a rotating anode generator. Data were collected using a Siemens Hi Star two-dimensional detector. Scanning electron micrographs were obtained on a Jeol 6320 SEM at a magnification of 75,000. The samples were cut with a razor blade and coated with sputtered gold. Sample densities were measured by weight change after immersion in water. Tensile properties (stress–strain and elastic recovery) were measured on a Q-Test 2-tensile machine (from MTS) using 50-mm-long samples and a 50 mm/min extension rate. Thermal measurements were carried out using a TA Instruments Thermal Analyst System consisting of the Controller 3100, DSC 2910, TMA 2940, and DEA 2970 modules. The heating rate was 5°C/min for all methods. Differential scanning calorimetry (DSC) was carried out in the modulated mode. Dynamic mechanical tests were carried out on a Rheometrix DMTA model Mark III at 5°C/min and 10 Hz. Dielectric tests were performed after two different pretreatments. In the first case samples were stored under ambient conditions prior to the test, while in the second they were thoroughly dried (heated to 70°C in vacuum for at least 24 h). Ambient or dry preconditioning is denoted by *a* and *d*, respectively.

RESULTS AND DISCUSSION

Structure and Morphology of Composites

The FTIR spectra of the pure nanosilica showed strong Si—O absorption at about 1,100 cm^{-1} and a small OH peak at 34,24 cm^{-1}. They also displayed a peak at 958 cm^{-1}, which was not observed in the pure microsilica. Th attenuated total reflection (ATR) spectra of pure polyurethane (PU) and composites with nanoparticles were essentially the same, except for the additional

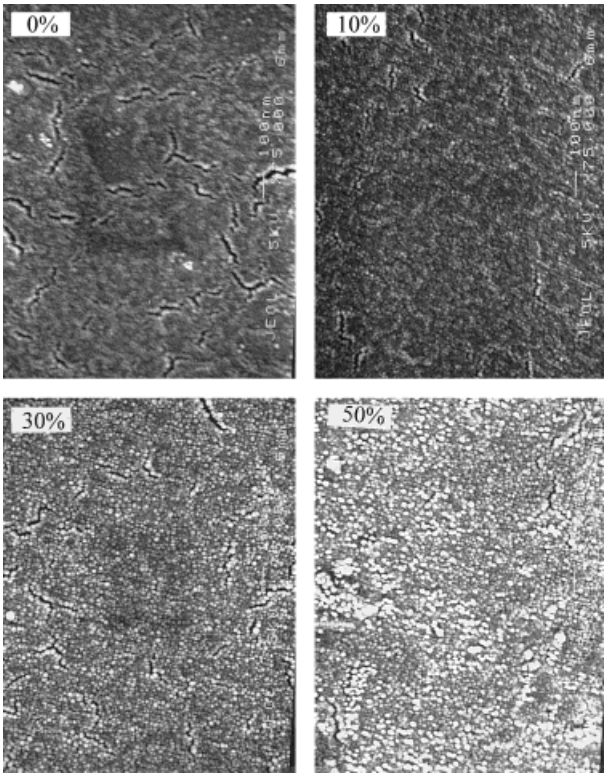

Figure 1 SEM micrographs of nanocomposites with different filler concentrations.

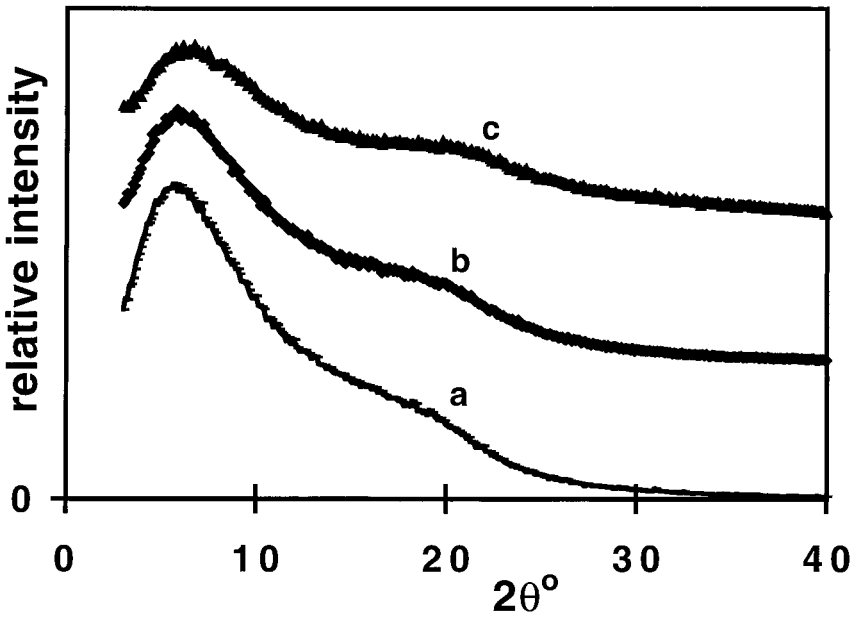

Figure 2 WAXD diffractograms of samples with (a) 0%, (b) 10%, and (c) 30% nanosilica.

bands of silica in the latter. Although an excess of 5% of isocyanate was used in all samples, IR spectra showed no free isocyanate peaks. It is assumed that some isocyanate reacted with OH groups from the filler, forming an organic–ceramic composite.

SEM micrographs of samples with 0 wt %, 10 wt % (5.5 vol %), 30 wt % (18.2 vol %), and 50 wt % (34.2 vol %) are shown in Figure 1.

Already with 10 wt % of nanosilica, the field appears pretty crowded with particles, which is even truer for samples with 30 wt % and 50 wt % filler. Particles are in the expected size range (i.e., 10–20 nm).

The WAXD of nanocomposites showed a lower angle peak, at about $2\theta = 6°$, and most showed a distinct shoulder at $2\theta = 20°$. Figure 2 displays the diffractograms of the samples with 0%, 10%,

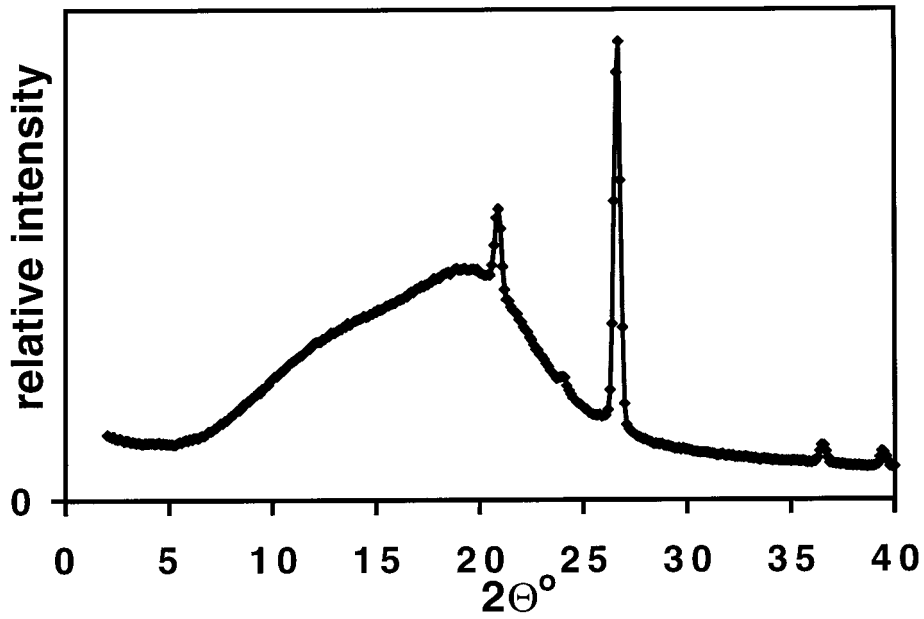

Figure 3 WAXD diffractogram of sample with 10% microsilica (quartz).

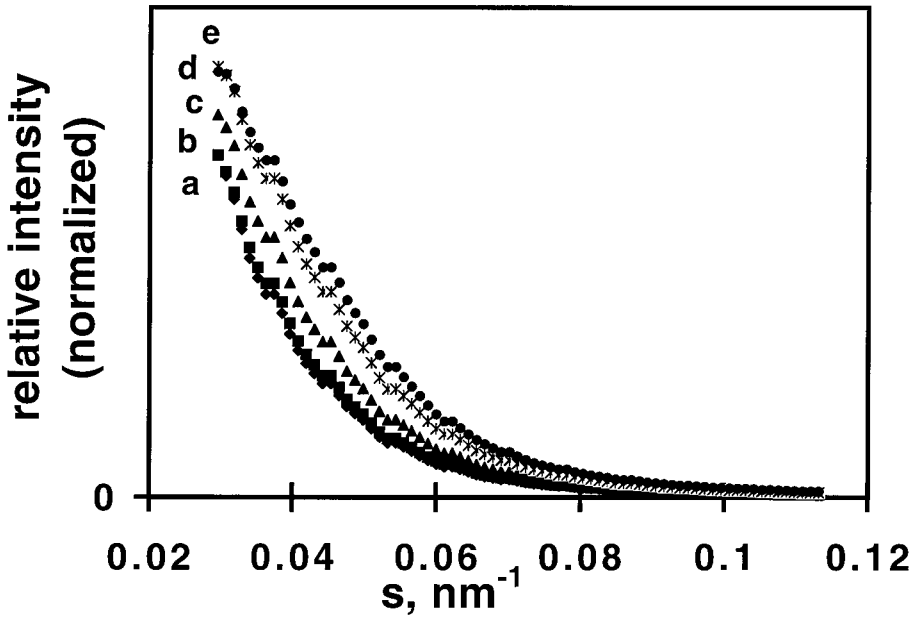

Figure 4 SAXS curves for samples filled with different concentrations of nanosilica. Data are plotted as I versus s. From bottom to top: (a) 10, (b) 20, (c) 30, (d) 40, (e) 50 wt % silica nanoparticles. Normalized intensities.

and 30% nanosilica. In samples with 20% and 50% filler, the shoulder is less obvious but evident nonetheless. It's considered that these broad peaks come from the polyurethane matrix. Clearly, the nanosilica did not display any crystalline peaks, which is consistent with the silica nanoparticles being noncrystalline at that size scale.

Materials with micron-size crystalline SiO_2, which were also examined with WAXD (10%, 30%, and 50% loading), displayed Bragg peaks at $2\theta = 20.9°$ and 26.7° (with spacing of 0.336 nm and 0.33 nm, respectively), corresponding to the most intense of known reflections of crystalline quartz. An example of this, for the 10% loaded sample, is shown in Figure 3. The SAXS results for samples with 10, 20, 30, 40, and 50 wt % nanospheres are shown in Figure 4. These are in the form of I versus s, where s is 2 sin θ/λ and I is intensity. Considerable absorption was observed with the highest SiO_2 content; however, in Figure 4 the intensities have been normalized to account for this, as described later.

None of these showed an obvious sharp interference peak, indicating the absence of a regular superstructural organization. However, Figure 4 does show some discontinuities in the smooth decay of I, with increasing s in all samples. These may possibly represent some very weak interparticle correlations.

Clearly, as the volume fraction of the nanospheres, V_f, increases, it is expected that they will eventually be forced by purely space-filling constraints to adopt a more regular packing. In the extreme situation where V_f approaches that for a close-packed array of spheres, we then expect the microspheres to form a lattice with well-defined lattice planes, which would produce well-defined Bragg peaks in X-ray diffraction, recognizable as sharp, discrete maxima. For close packing of regular spheres into a lattice, the theoretical value of V_f is 0.74. Clearly, we have not reached this point. Our values of V_f were always far below that for a close-packed system (see Table II); in addition, the nanospheres themselves have some distribution in size, therefore disrupting the regularity of packing.

The absence of any relevant interparticle interference pattern allowed us to analyze the SAXS profiles in terms of the scattering from single particles. The analysis was carried out using the Gaussian approximation to the Guinier scattering regime,[16] which states, as is well known, that the scattered intensity, $I(s)$, decreases with s according to

$$I(s) = I_0 \exp(-(4/3)(\pi^2 R_g^2 s^2)) \qquad (1)$$

where I_o is the scattered intensity at zero angle and R_g is the electronic radius of gyration.

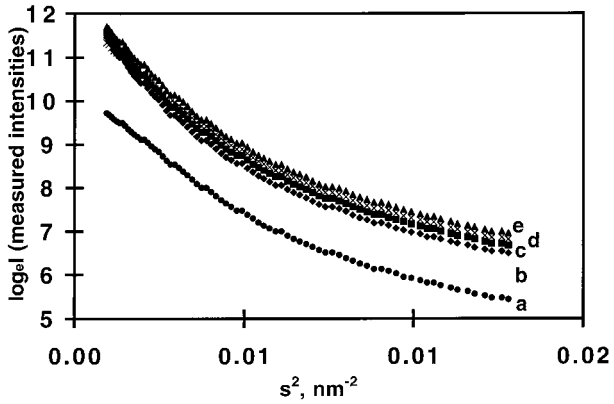

Figure 5 Guinier plots for nanocomposites. From bottom to top (a) 50, (b) 10, (c) 20, (d) 40, and (e) 30 wt %. Experimentally recorded intensities.

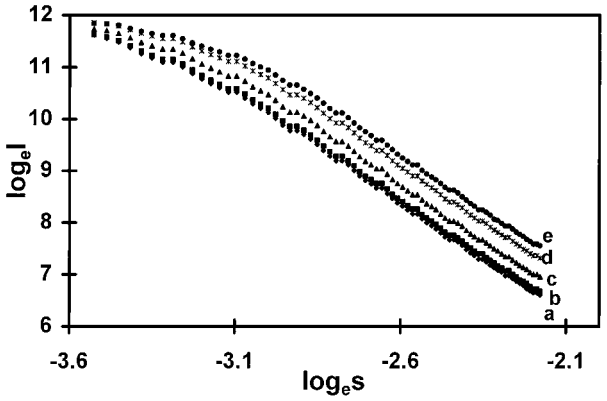

Figure 6 Log $_e(I)$ plotted against log $_e(s)$ for nanocomposites to test for validity of Porod's law: (a) 10, (b) 20, (c) 30, (d) 40, and (e) 50 wt % silica.

Figure 5 shows plots of log $_eI$ versus s^2 over the whole range of s for all the materials. The fit is linear for low values of s^2, which is the range of validity of the Guinier approximation. In fact, the range of linearity increased to a larger s at higher loadings. Values of R_g calculated from this are shown in Table I. Assuming that the scatterers are spherical in shape, the geometrical radius, r, is related to R_g by:

$$R_g = r(3/5)^{1/2} \quad (2)$$

Values of r are also shown in Table I. In all cases except 50% loads, the volume of equivalent solid spheres estimated by SAXS exceeded the volume measured by SEM and was at the high end of the manufacturers' quoted size range (10–20 nm in diameter).

The extrapolation of the linear fit in the Guinier range to the ordinate axis allowed an estimation of log $_e(I_o)$, which therefore enabled the normalization of intensities in cases where absorption effects were significant.

Table I Values of the Electronic Radii of Gyration, R_g, and the Corresponding Radii of Solid Spheres, r

Filler Volume Concentration V_f (%)	R_g (nm)	r (nm)
10	8.4	10.9
20	8.3	10.7
30	7.8	10.1
40	7.1	9.2
50	6.8	8.8

The data were also examined for their correspondence to Porod's law,[17] which states that with pinhole collimation, the product $I.s^4$ approaches a limiting value in the high-angle tail of the SAXS curve, that is, lim $(I.s^4) = k_p$, where k_p is the Porod constant. The extent of this law's validity for the nanocomposites can be seen from Figure 6, in which plots of log $_e(I)$ versus log $_e(s)$ are linear for log $_e(s) > \sim -3.0$ ($s > \sim 0.05$ nm^{-1}); these plots were made using normalized intensities as described above.

In all cases the values of the slopes obtained by regression analysis were ~ -4.3 rather than -4.0. Such deviations from ideal Porod behavior may imply the presence of density fluctuations within one of the phases (probably the PU matrix in this case). The value of the Porod constant, k_p, is obtained from the intercept on Figure 6 and is theoretically proportional to the total interfacial area in the system. In the absence of aggregation effects, this should scale with the silica content. Figure 7 shows that this is indeed the case, with the data generally falling on a straight line that passes through the origin of the plot (although the value for the sample with the lowest loading does appears to be rather high).

The ratio of k_p to the scattering power of the system is proportional to the specific inner surface, that is, the surface-area-to-volume ratio of the dispersed phase. For the constant shape of the filler particle, this is expected to be independent of volume fraction. The scattering power itself is proportional to the mean square fluctuation of the electron density, $(\Delta\rho_e)^2$, which in a two-phase system is given by

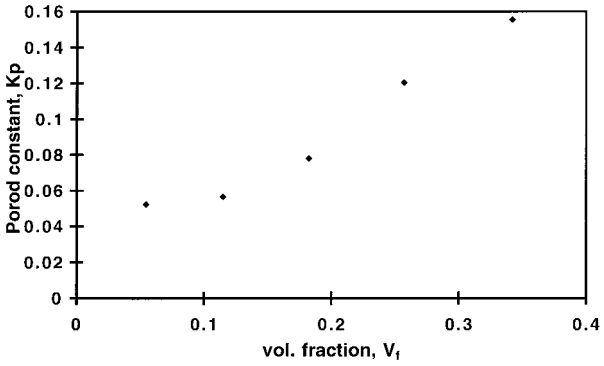

Figure 7 Values of Porod constant, k_p, obtained from Fig. 6 for nanocomposites.

$$(\Delta\rho_e)^2 = (\rho_{e1} - \rho_{e2})^2\phi_1\phi_2 \quad (3)$$

where ρ_e is the electron density per volume and ϕ_i is the volume fraction of the ith phase. It is straightforward to estimate the electron densities for both the dispersed silica and the PU matrix phases. The density of the silica was estimated at 2.3 g/cm^{-3} (see later) and the density of the PU was taken as 1 g/cm^{-3} leading to values of 1.11 and 0.57 mol electrons cm^{-3}, respectively, for the electron densities. Table II shows the value of the ratio of $k_p/(\Delta\rho_e)^2$ for all the nanocomposites. For materials with 20, 30, and 40 wt % loading, the ratio is reasonably constant, while for the 50 wt % samples, the value is slightly larger. This may reflect a decrease in the electron density difference in this sample. The considerably larger ratio for the 10 wt % sample is probably due to an overestimation of the value of k_p, (Fig. 7).

Physical and Mechanical Properties

According to the linear mixture equation (LME), the density of a composite, ρ_c, is a linear combination of densities of the matrix, ρ_m, and filler, ρ_f, and their respective volume fractions, ϕ_m and ϕ_f:

Table II Ratio of $k_p/(\Delta\rho_e)^2$ for Nanocomposites

Weight Concentration (wt %)	Filler Volume Fraction	$k_p/(\Delta\rho_e)^2$
10	0.0546	3.54
20	0.115	1.95
30	0.1822	1.83
40	0.257	2.13
50	0.342	2.41

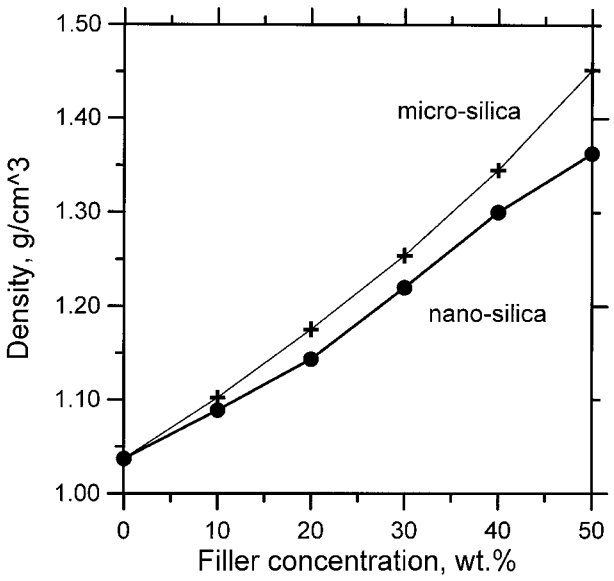

Figure 8 Effect of filler concentration on density of polyurethanes filled with microsilica and nanosilica.

$$\rho_c = \rho_m\phi_m + \rho_f\phi_f \quad (4)$$

The density of the samples increased with filler concentration in both series, but more so in the series with microsilica (Fig. 8). Using the LME, the extrapolated densities were calculated to be 2.0 g/cm^3 for nanosilica and 2.48 g/cm^3 for microquartz, respectively. The accepted value for the density of quartz is 2.65 g/cm^3. The density of the original 30% solution of nanoparticles in MEK was given to be 0.98–1.02 g/cm^3. Since the density of MEK is 0.805 g/cm^3, it follows that the calculated density of particles should be 2.3 g/cm^3. The difference between the density of nanoparticles in MEK and the apparent density in polyurethane is too large to be explained by the lowering of density of the matrix due to incomplete curing, because the latter is not very different from that of uncrosslinked polyols. It appears that incorporation of nanoparticles somehow increases the volume of the polymer matrix.

The interaction between matrix and filler can be assessed from the shift of glass transition with increasing filler concentration. It has already been observed that the polyol has a strong interaction with the nanoparticles, but that may be offset by incomplete curing for similar reasons. To examine the degree of curing, we carried out swelling tests. The degree of swelling—calculated as the ratio of the volume of swollen polymer (polymer + solvent but no filler) to the volume of

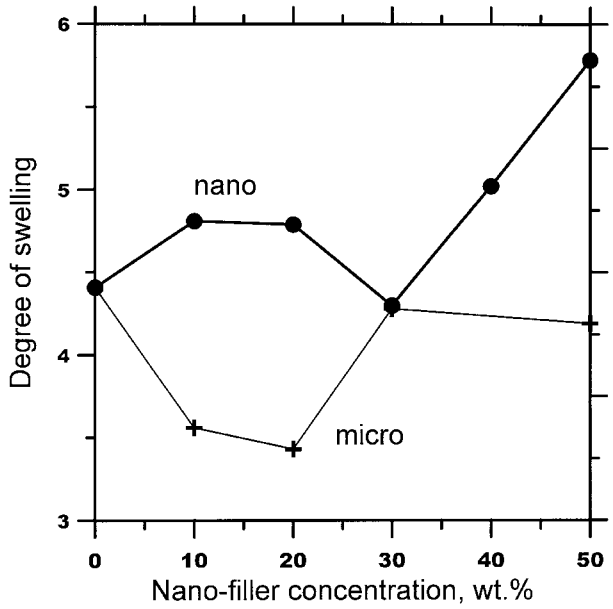

Figure 9 Degree of swelling of nanocomposites and microcomposites.

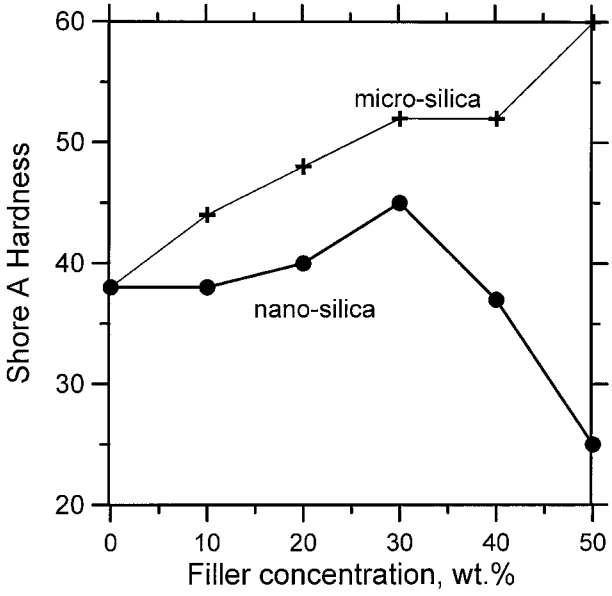

Figure 10 Shore hardness of nano- and microcomposites.

the polymer (without filler) before swelling—for two series of composites is shown in Figure 9. Since a lower degree of swelling indicates better curing, it is obvious that the sample with 50% nanosilica stands out as less cured, while the results for other samples oscillate within the experimental error.

Values of T_g from the reversible heat flow, obtained by modulated DSC, were around −50°C and did not display strong dependence on the filler content or the type of filler. However, TMA, DMTA, and DEA measurements indicated that T_g increased with increasing filler concentration both in nanocomposites and microcomposites, and it was somewhat faster in the former (Table III). T_g from DMTA measurement was obtained from the maximum on E″-versus-temperature curve and in DEA from the loss factor(ε'') maximum.

Different methods gave somewhat different results, but it is evident that an increase in T_g of about 10°C occurred when the concentration of nanospheres increased from 0% to 50 wt %. The increase in T_g for the micron-size silica–filled polyurethanes was somewhat smaller. It appears that although there was a strong interaction between the matrix and the filler (which should have increased T_g), an opposing effect came from incomplete curing of the matrix.

Hardness is a basic property characterizing elastomers. The Shore A hardness of the samples increased steadily with increasing microsilica concentration, but with nanosilica this decreased after an initial increase (Fig. 10). Obviously, mi-

Table III Glass Transition Temperatures for Two Series of Composites as Measured by TMA, DMTA at 10 Hz, and DEA at 1 Hz

Filler Conc (wt %)	T_g (TMA) (Nanocom. °C)	T_g (TMA) (Microcom °C)	T_g (DMTA) (Nanocom. °C)	T_g (DMTA) (Microcom. °C)	T_g (DEA) (Nanocom. °C)	T_g (DEA) f (Microcom. °C)
0	−51.5	−51.5	−49	−49	−45	−45
10	−51	−47	−46	−47	−44	−43
20	−51	−50	−42	−43	−43	−43
30	−48	−50	−41	−43	−40	−40
40	−43	−50	−39	−40	−39	−44
50	−51	−47	−38	−39	−35	−40

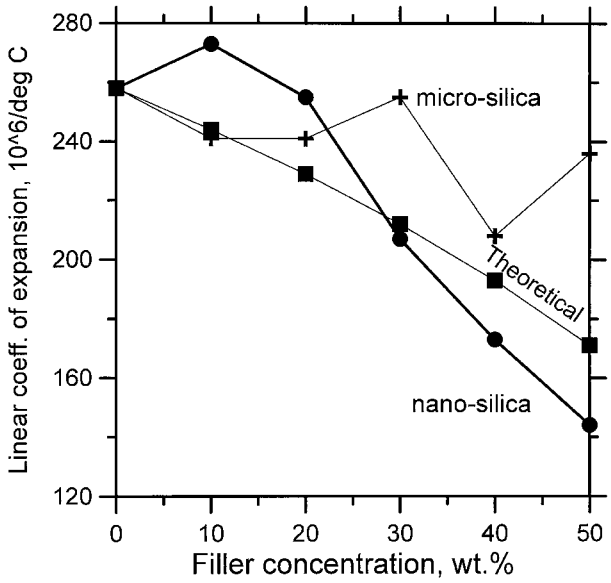

Figure 11 The effect of filler concentration on linear thermal expansion coefficient of nano- and microcomposites.

crosilica is a hard filler, while it appears that nanosilica is not. It is interesting to note, however, that some authors have found increased hardness and scratch resistance with the addition of nanoparticles.[18]

One parameter allowing an estimate of interaction is thermal expansion. According to Kerner,[19] the volume thermal expansion coefficient of a composite filled with spherical particles varies nonlinearly with the volume fraction of the filler and matrix (ϕ_f, ϕ_m)

$$\beta_c = \beta_m\phi_m + \beta_f\phi_f - (\beta_m - \beta_f)\phi_m\phi_f\theta \qquad (5)$$

where β_c, β_m, and β_f– are volume coefficients of expansion of the composite, matrix, and filler, respectively, and θ is a parameter depending on the bulk moduli of the matrix and filler, K_m and K_f, and the shear modulus of the matrix, G_m:

$$\Theta = \frac{(1/K_m) - (1/K_f)}{(\phi_f/K_m) + (\phi_m/K_f) + 3/(4G_m)} \qquad (6)$$

The third term in eq. (5) is usually small with round particles, and the behavior can be reasonably well described by the LME [the first two terms in eq. (5)]. Figure 11 shows the change of the linear coefficient of expansion at 60°C, α, with concentration of both fillers. A lower α for nanocomposites may reflect a stronger interaction with the matrix.

The modulus of a composite is a function of the moduli of the matrix and the filler. Several models for predicting the modulus of a composite are available.[20] The change of storage modulus of samples with nanosilica with temperature is shown in Figure 12, and the change with microsilica is shown in Figure 13. Both figures show the increase in modulus with increasing filler concentration in the glassy and rubbery state. This change was less regular in the nanocomposites, where the curing reaction was more affected by the presence of the filler.

Direct comparison of the moduli in the rubbery state of samples with the same concentration of nanosilica and microsilica showed generally higher values for nanocomposites at 40% and 50% filler, but the reverse was observed at lower filler concentrations. The stress at 100% elongation (100% modulus) was generally lower in the nanosilica-filled composites. The variation of modulus with concentration was fairly irregular and was not amenable for modeling.

The tensile strength of the composites with nanosilica and microsilica, shown in Figure 14, indicated that up to a 20% filler concentration there was not much difference between the nanosilica and microsilica effect. However, at higher concentrations the nanosilica made the composites three times stronger, while the strength of the microsilica-filled composites decreased, a finding that should be considered in conjunction with elongation at break (Fig. 15). Although the microsilica slightly increased the elongation at break, the nanosilica showed a 600% improvement. Experiments with nanosilica in PDMS elastomers showed that the elongation decreased and strength increased with increasing filler concentration.[8] On the other hand, nanotitania-filled PDMS networks showed partial increase in elongation at break with increasing filler content—that is, no regular pattern can be said to be emerging.[21]

The elastic recovery was measured at 100% elongation in the cycling elongation test. It was found that all samples recovered around 95% of elongation, except for the sample with 50% nanosilica, which showed 85%–90% recovery. However, the same sample displayed a stress increase in the second cycle at about 5% deformation; that is, it showed the same recovery as the other samples, but it took longer. The polyurethane with 50% microsilica displayed stress softening in the

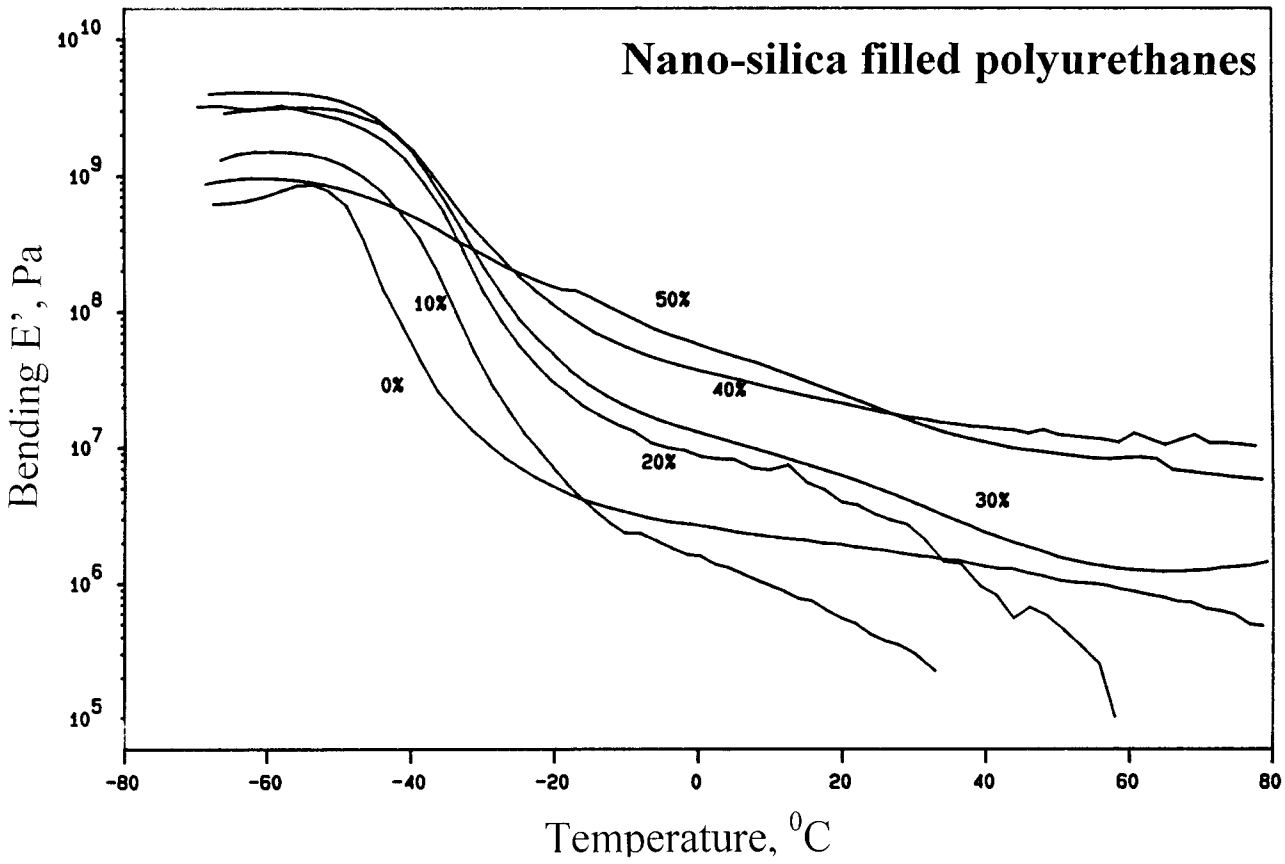

Figure 12 Effect of temperature on storage modulus of nanocomposites.

repeated cycles, while the corresponding nanosilica-filled sample had the same shape of the curve in the second cycle. Hysteresis in all samples was rather small except for samples with 50% nanosilica and microsilica. The rebound resilience of all composites decreased with increasing filler concentration and was lower in nanocomposites than in microcomposites.

Optical Properties

Polyurethane–nanosilica composites were transparent at all filler concentrations, while those with microsilica were not. The refractive indices of the matrix and filler seemed to be similar since the refractive index of the composites decreased from $n^{23} = 1.478$ for the pure matrix to only 1.474 for the composite with 50% nanosilica. UV/VIS spectra of 1-mm-thick samples showed total absorption below 320 nm and high transmission between 450 and 900 nm in all samples with nanosilica.

Dielectric Properties of Nano- and Microcomposites

Dielectric spectroscopy (DEA, dielectric analysis) is a powerful tool in studying relaxation phenomena in polymers and composites.[22,23] It may provide us with information about the location and activation energy of relaxation transitions, the dipole moment of the subunits involved, concentration and mobility of charge carriers, and so forth. To get a complete view, it may be combined with other mechanical, thermal, and spectroscopic (IR, NMR, etc.) techniques.

DEA data comprise dielectric permittivity (ε') and loss (ε''), which are defined as

$$\varepsilon^*(\omega) = \frac{D(\omega)}{E(\omega)} = \varepsilon' - i\varepsilon'' = \varepsilon' - i\left(\varepsilon_d + \frac{\sigma}{\varepsilon_0\omega}\right) \quad (7)$$

where D is the displacement, E is the electric field, ω is the radial frequency, ε''_d denotes the dipolar part of the dielectric loss, σ is the ohmic

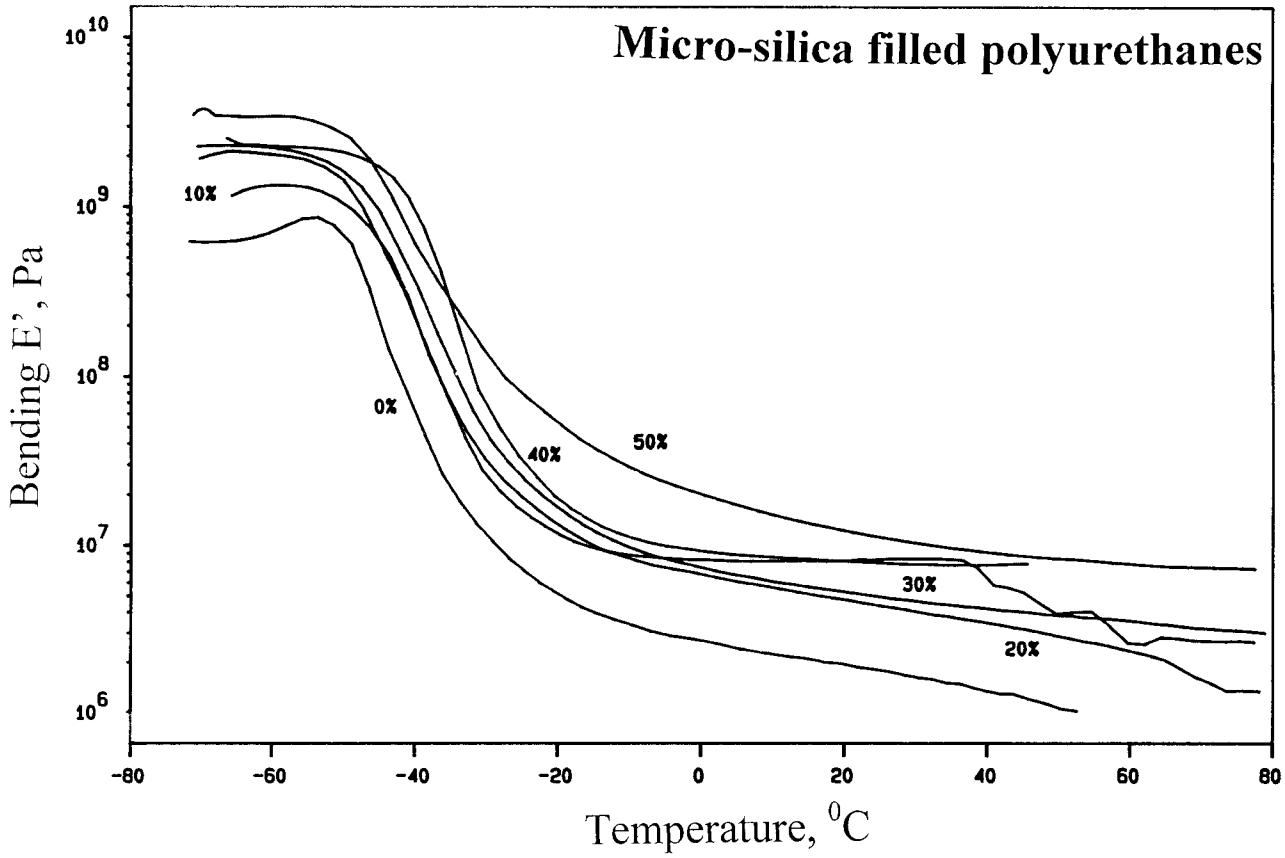

Figure 13 Effect of temperature on storage modulus of microcomposites.

conductivity, and ε_0 is the vacuum permittivity. Dielectric loss is frequently presented as tan δ, which is defined as:

$$\tan \delta = \varepsilon''/\varepsilon' \quad (8)$$

Dielectric data are plotted either versus log frequency, using temperature as a parameter, or versus temperature, using log frequency as a parameter. Transition temperatures are usually plotted as log f_{max} versus 1/T, and from the slope of this plot, the activation energy of the dielectric relaxation can be estimated. Electrical properties of nanocomposites have only recently begun to be studied. Some interesting effects of particle size were observed when the dielectric constant of a polymer–lead titanate composite with particles smaller than 200 nm showed a sharp reduction.[24]

Silica typically has permittivity of about 3.3 at room temperature,[25] while our polyurethane has ε' of about 3.0 in the glassy state and about 6.0 in the rubbery state at 1 kHz.

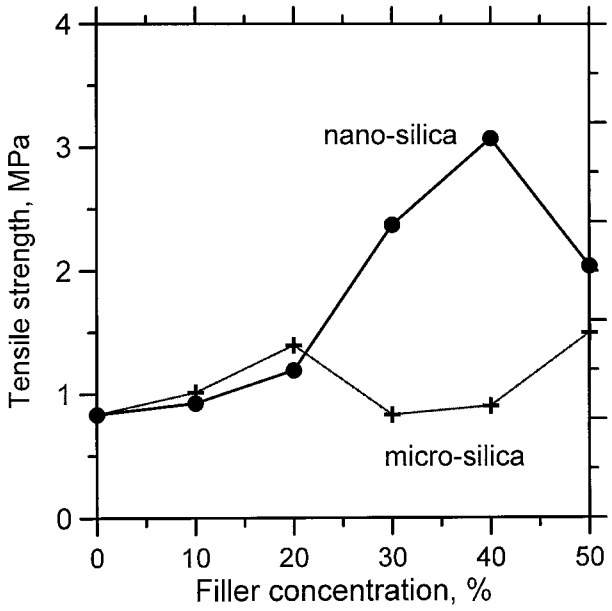

Figure 14 Dependence of tensile strength on filler concentration of nano- and microcomposites.

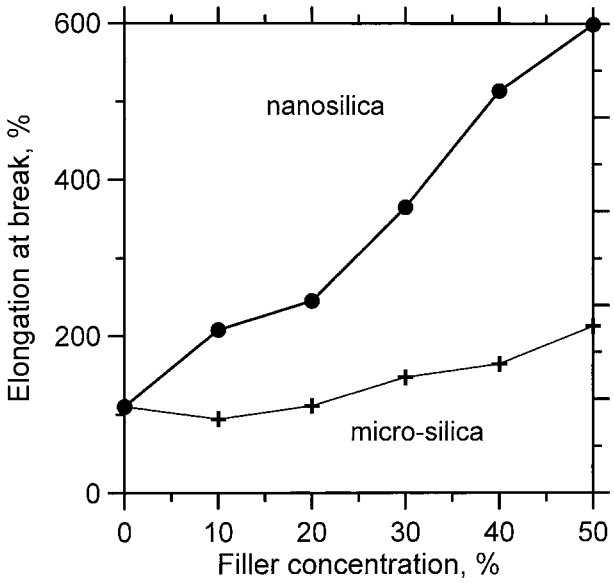

Figure 15 Dependence of elongation at break on filler concentration of nano- and microcomposites.

Figures 16 and 17 show the dielectric permittivity and tan δ of a typical composite (PUR/micro 30 a). Samples are designated as PUR/nano xx, where *xx* denotes the filler content in weight percentage.

The permittivity curves (Fig. 16) exhibit one major transition, which becomes broader at higher frequencies. The onset of a new polarization mechanism are visible at frequencies lower than 100 Hz. Taking into account the heterogeneous nature of the system (polymer matrix + filler), this might be interpreted as a Maxwell–Wagner–Sillars (MWS) polarization,[23] but there are reasons that this may not be so. First of all, the increase of ε' at lower frequencies and higher temperatures appears in the nonfilled sample as well, in spite of the polyurethane not being phase separated. Also interesting is the apparent equilibrium polarization of this new polarization mechanism, which seems to depend on the measuring frequency. These characteristics are more in agreement with an electrode polarization mechanism (electrode blocking) than with MWS polarization.

The tan δ curves (Fig. 17) indicate a gradually dominant role of conduction in determining the loss with decreasing frequency. A broadening of the transition can be observed with increasing frequency, which agrees with the data in the per-

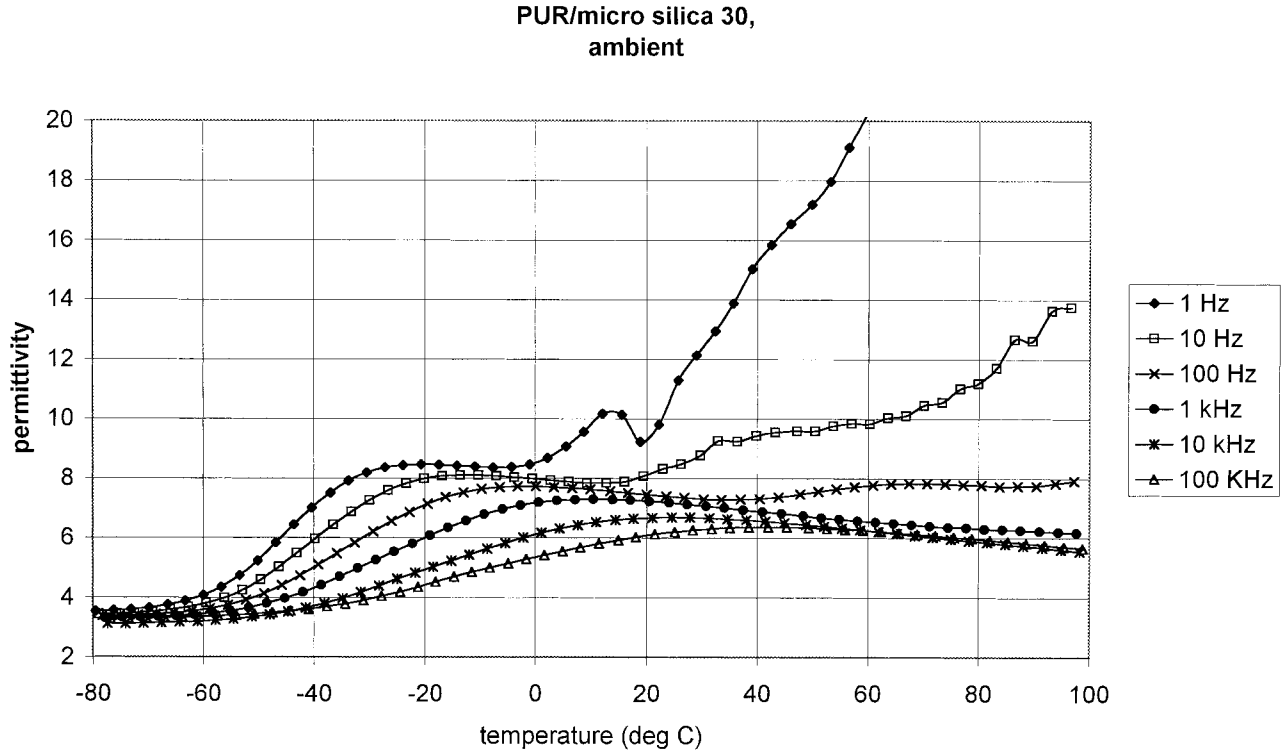

Figure 16 Dielectric permittivity (ε') curves of a polyurethane composite containing 30 wt % microsilica filler. The sample was stored under ambient conditions.

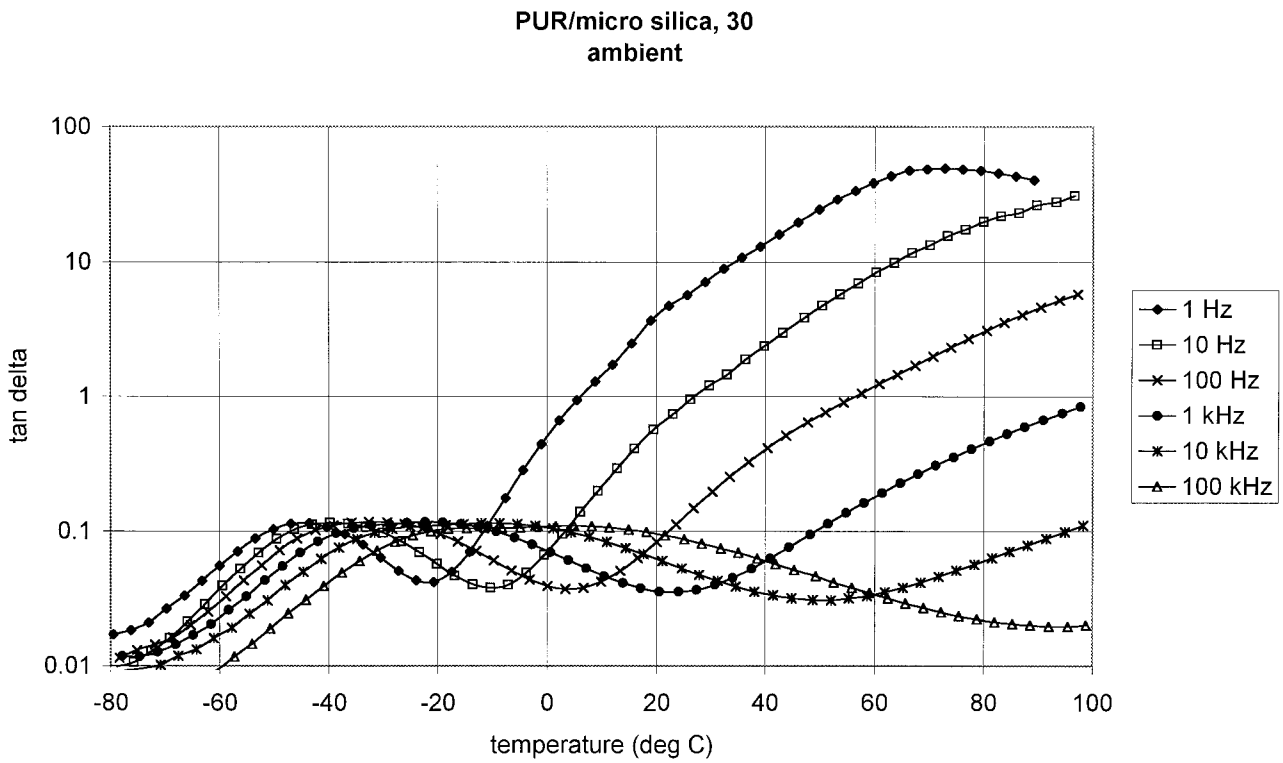

Figure 17 Dielectric tan δ curves of a polyurethane composite containing 30 wt % microsilica filler. The sample was stored under ambient conditions.

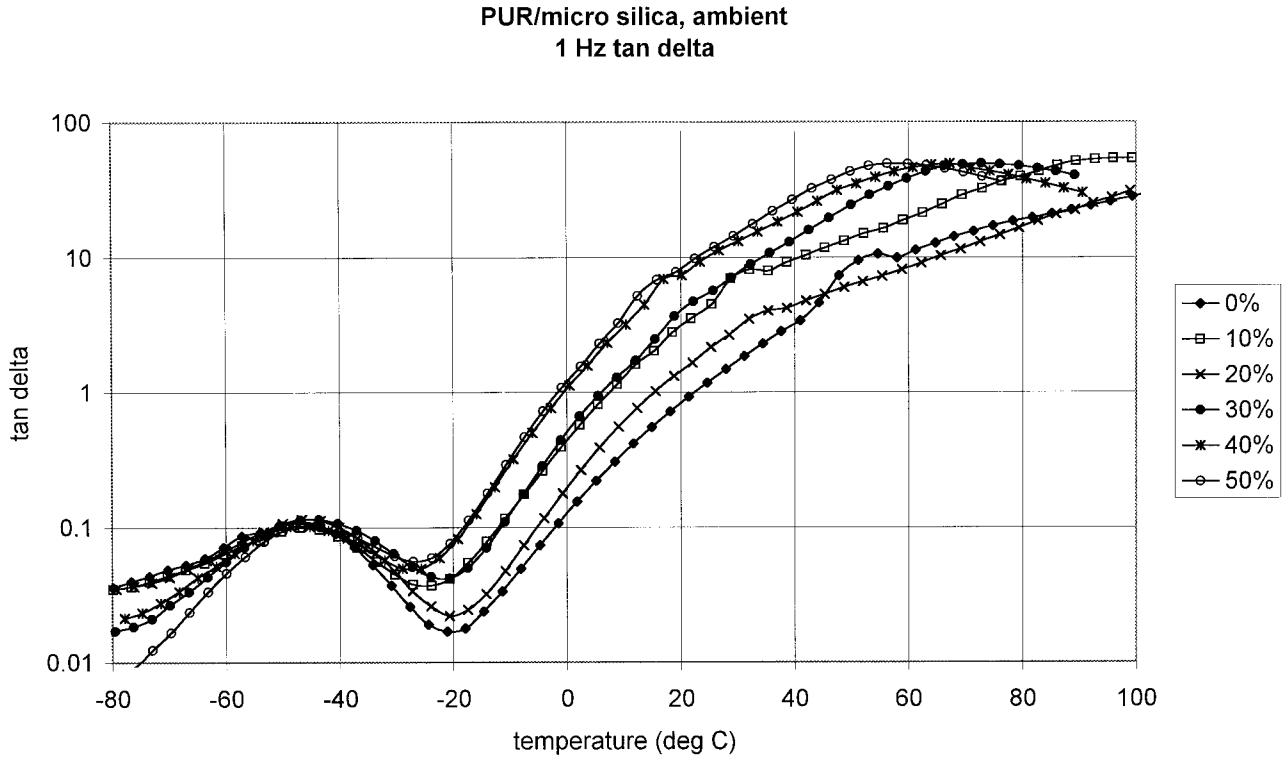

Figure 18 1 Hz tan δ curves of polyurethane composites containing various amounts of microsilica filler. The samples were stored under ambient conditions.

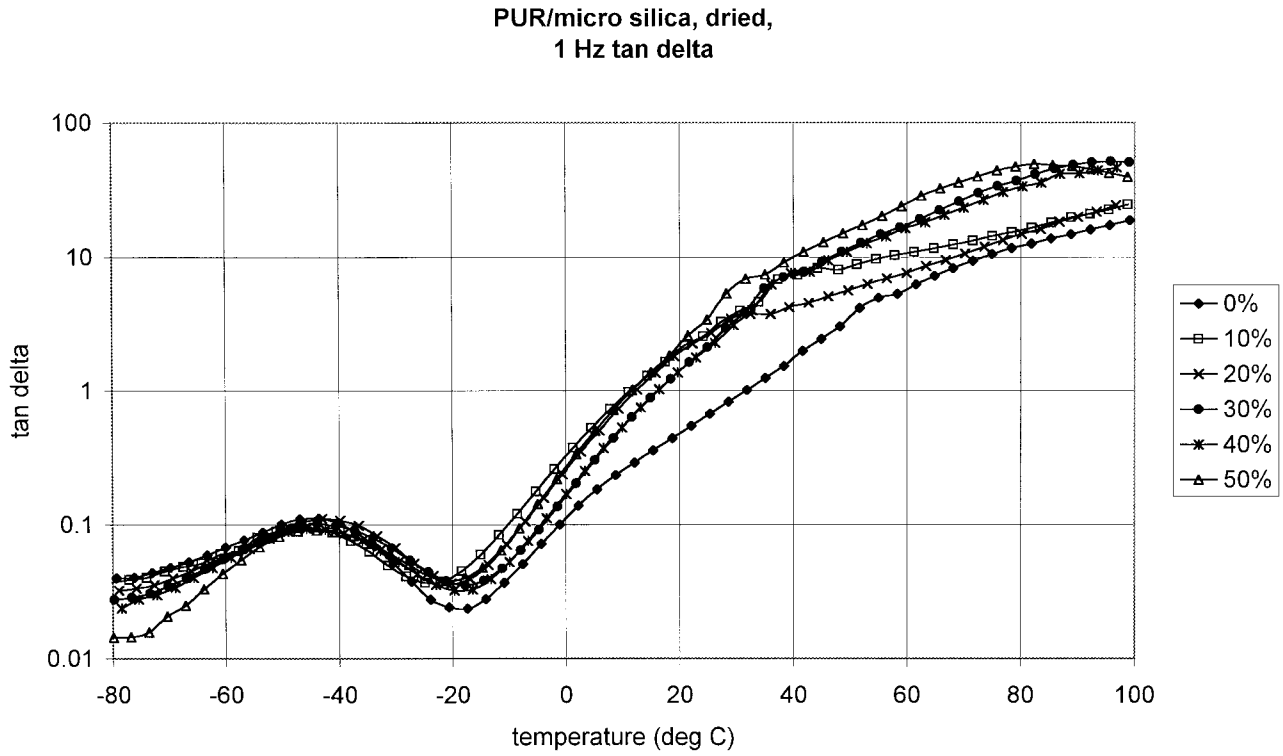

Figure 19 1 Hz tan δ curves of polyurethane composites containing various amounts of microsilica filler. The samples were thoroughly dried prior to the measurement.

mittivity curves. As is demonstrated later in the article, at 100 kHz a doubling of the transition can be clearly discerned. The change of resolving power with measuring frequency is well known in dielectric spectroscopy, and it is explained by the nonuniformity of activation energies of various transitions. Usually the size of relaxation units increases with the transition temperature; therefore, in most cases the activation energy of the transitions increases with the transition temperature. This results in higher resolution power at lower frequencies. In our case, however, the opposite is true; therefore, the activation energy of the higher temperature transition is lower. As the transitions overlap, even at 100 kHz, the activation energies of the subtransitions can be estimated only roughly. The estimated values are 180–200 kJ/mol for the lower temperature transition and 90–110 kJ/mol for the higher temperature transition.

In order to compare the effect of various fillers on the dielectric behavior, the minimum (1 Hz, Figs. 18–21) and the maximum (100 kHz, Figs. 22–25) frequency tan δ curves have been selected. The first group is shown in logarithmic representation, as the conductivity-dominated tan δ values spread over several decades.

A comparison of the low-frequency data measured on samples stored under ambient conditions with those dried thoroughly prior to the measurement shows that water exerts a profound effect on the conductivity of the composites. This is not unexpected, as water may dissociate in the PU matrix, and the protons may contribute to the protonic conduction usually present in polyamides and in polyurethanes. In the dried samples the 1-Hz tan δ curves are much closer to each other than in the ambient-dried ones. In the samples stored under ambient conditions, the conductivity in general increases with the filler content, although the dependence is not monotonic. The tan δ curves exhibit a second maximum in the nanosilica-filled samples stored under ambient conditions. It can be speculated that this very high specific surface area filler collects the water more effectively at the filler–matrix interface; thus, it is possible that a true interfacial polarization appears because of the enhanced surface conductivity of the wet particles.[26]

The high-frequency data are almost totally free of conductivity effect, although the beginning of the conductivity tail appears with highly filled samples stored under ambient conditions. Drying diminishes these effects further. The relaxation

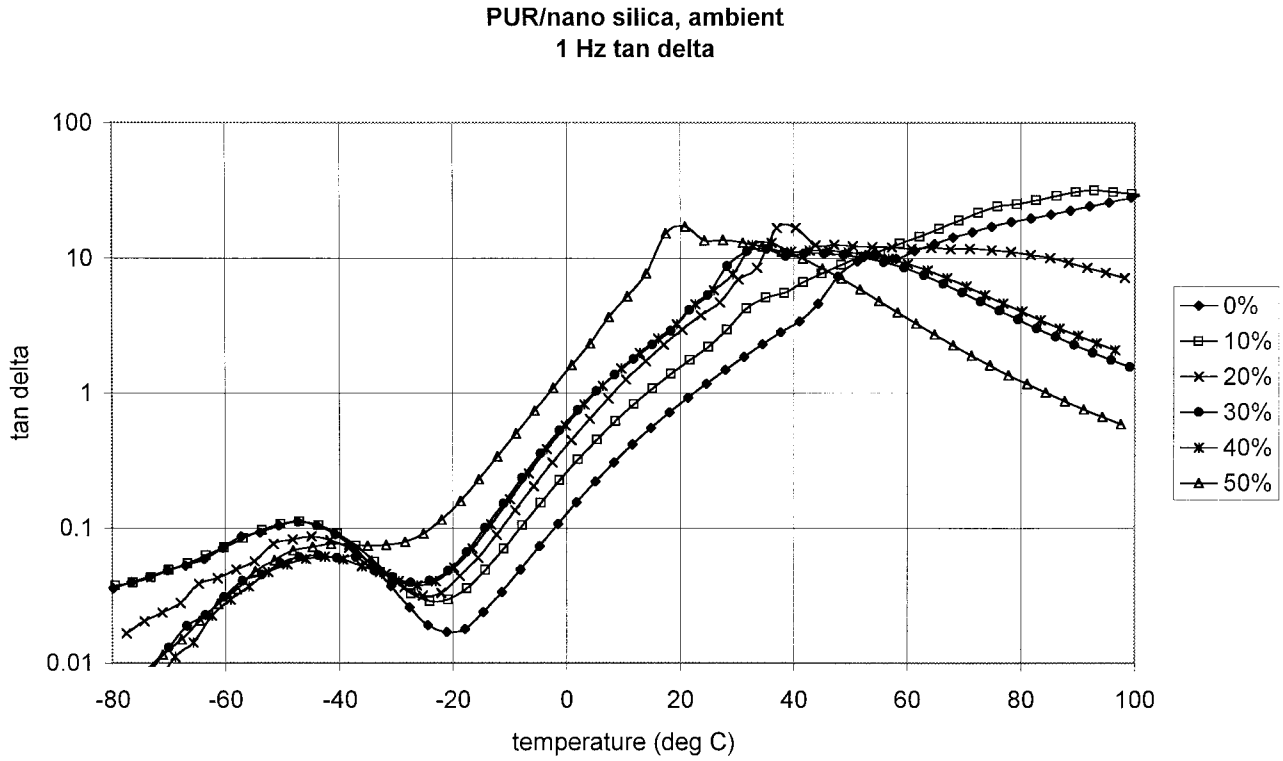

Figure 20 1 Hz tan δ curves of polyurethane composites containing various amounts of nanosilica filler. The samples were stored under ambient conditions.

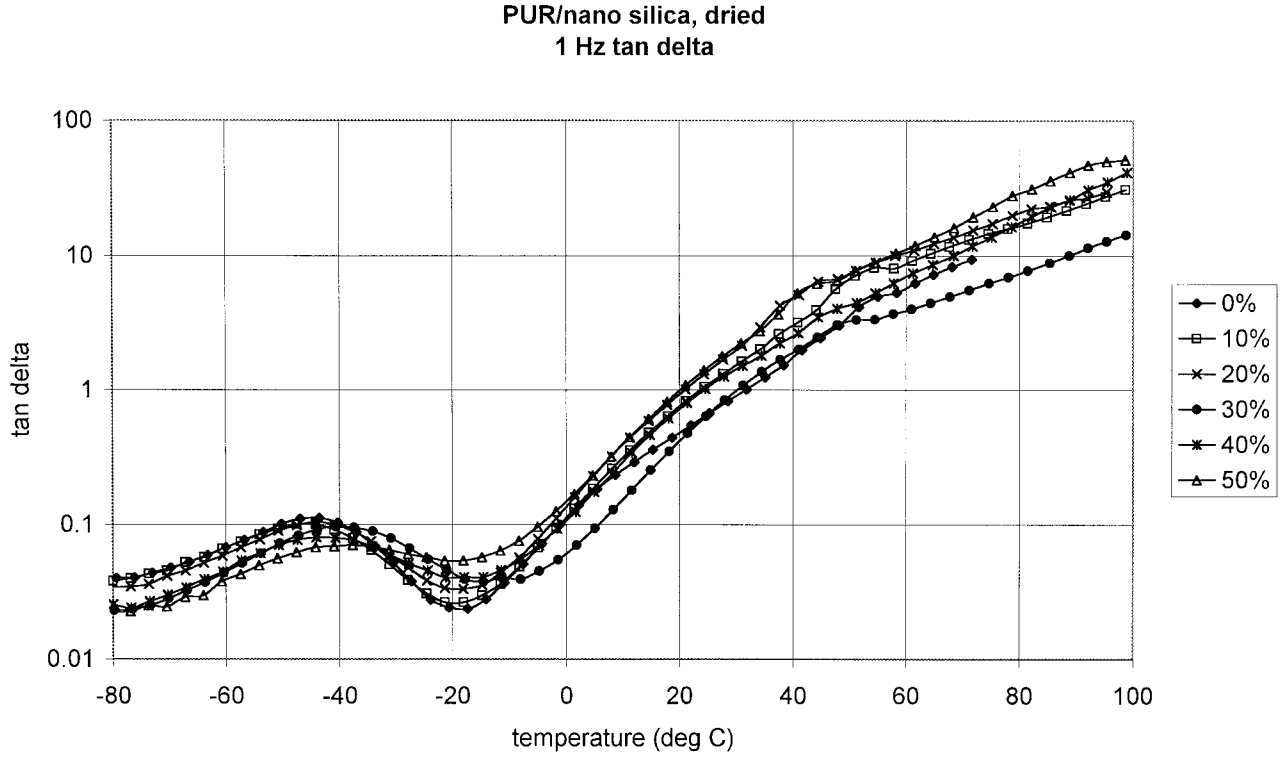

Figure 21 1 Hz tan δ curves of polyurethane composites containing various amounts of nanosilica filler. The samples were thoroughly dried prior to the measurement.

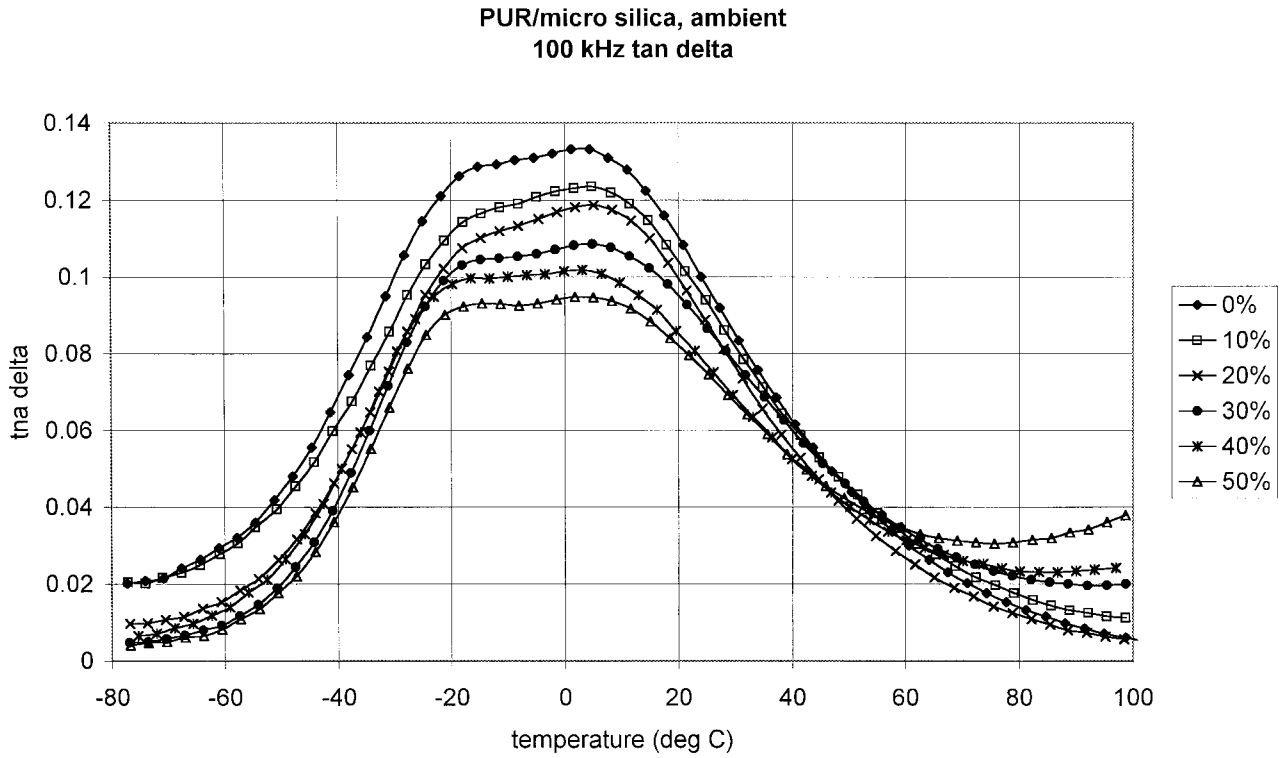

Figure 22 100 kHz tan δ curves of polyurethane composites containing various amounts of microsilica filler. The samples were stored under ambient conditions.

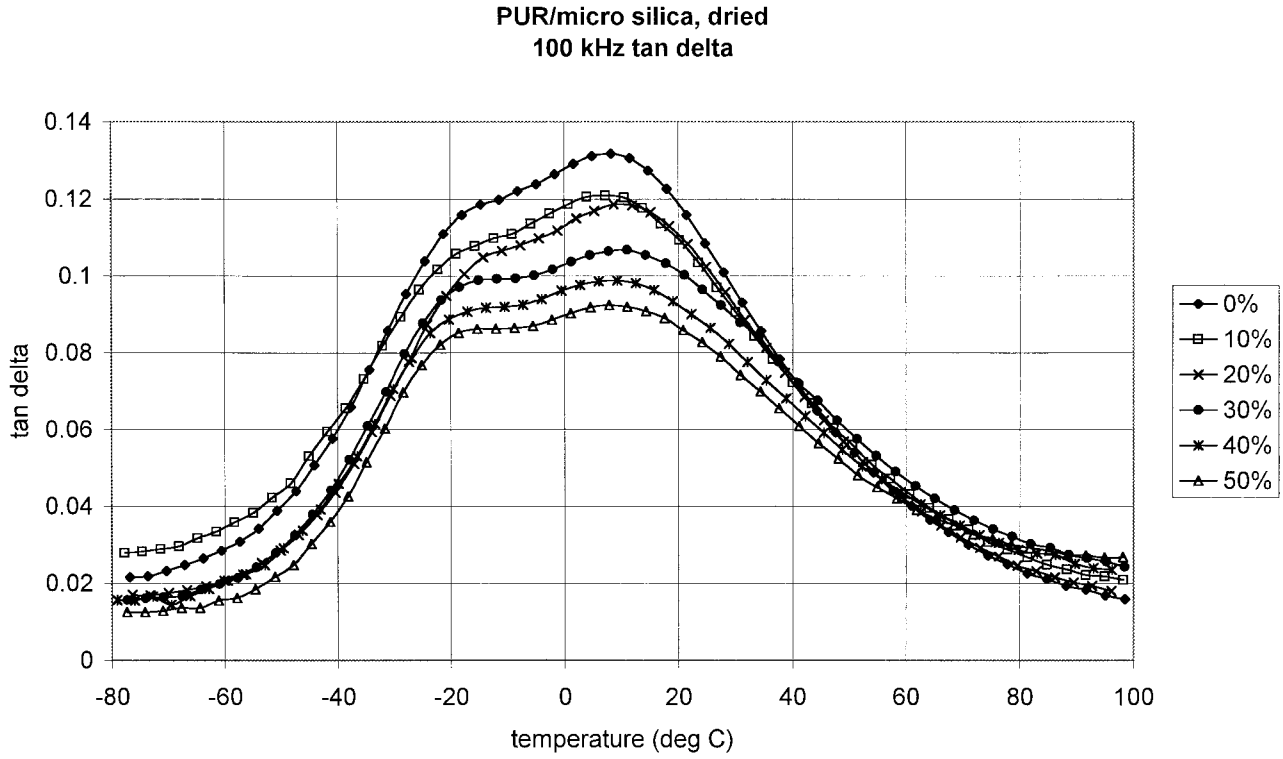

Figure 23 100 kHz tan δ curves of polyurethane composites containing various amounts of microsilica filler. The samples were thoroughly dried prior to the measurement.

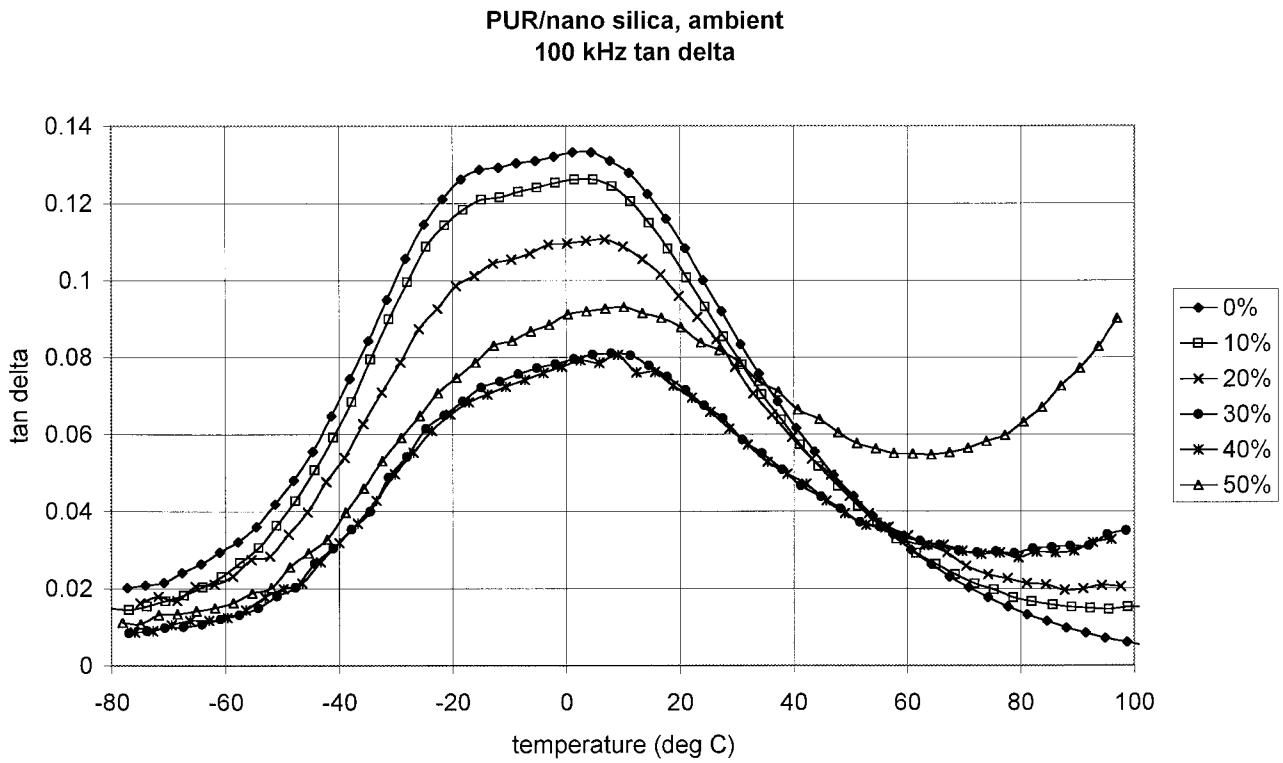

Figure 24 100 kHz tan δ curves of polyurethane composites containing various amounts of nanosilica filler. The samples were stored under ambient conditions.

strength (which is roughly proportional to the loss maximum) decreases with filler content in every case, which is the logical consequence of the "dilution" of dipoles by the dielectrically inactive silica filler. If the effect of conductivity is taken into account, the decrease of the relaxation strength with filler content is monotonic. This decrease is somewhat more pronounced with nanosilica filler, which can be understood in terms of minor density differences. A slight change in the relative intensity of the two subtransitions can be observed between the samples stored under ambient conditions and those dried thoroughly. With well-dried samples, the lower temperature transition is somewhat less intense than with ambient storing conditions. The origin of the doubled peak itself is not fully clear. This transition is basically the glass transition of the soft segment of the polyurethane, and the peak doubling cannot be attributed to adsorbed and free chains, as it appears not only in the filled samples, but in the pure PU sample as well. We may speculate that although there is no phase separation in the PU matrix, the soft segments located near the isocyanate groups behave differently from those far from them, and this may explain the existence of a doubled transition, with two different transition temperatures. The presence of water seems to influence this delicate balance, although the shift of the transition temperatures is negligible. Also interesting is that in the microsilica-filled samples the transition temperatures are almost totally independent of the filler content; in the nanosilica-filled samples the transition temperatures shift toward higher temperature with increasing filler content. This seems to corroborate our earlier observation that the nanosize filler exhibits closer interaction with the matrix than the microsilica filler. A comparison of the 100 kHz tan δ values of the dried samples shows that the interaction of the nanofiller is also probably more intense with water, as shown by the higher residual loss after drying at high temperatures.

CONCLUSIONS

Nanosilica filler is amorphous, making composites with polyurethanes, which were transparent at all concentrations. Such composites displayed higher strengths and elongation at break and

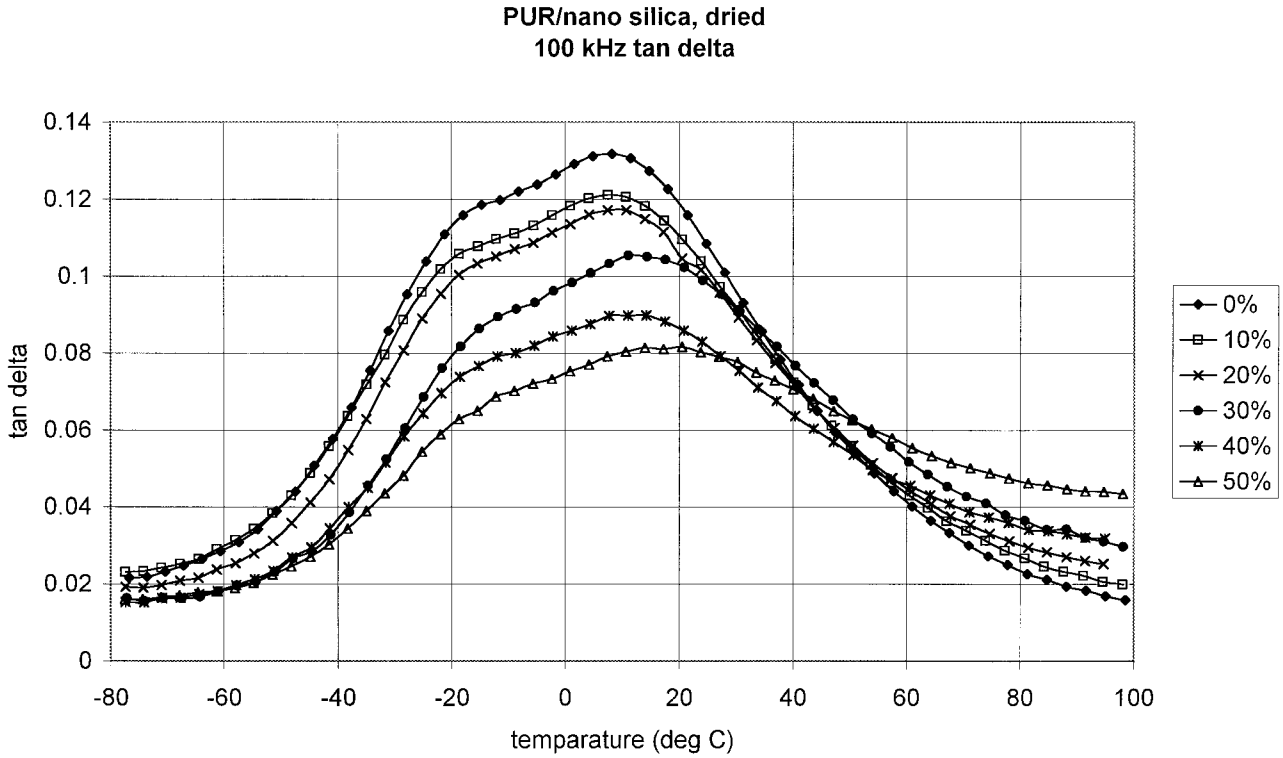

Figure 25 100 kHz tan δ curves of polyurethane composites containing various amounts of nanosilica filler. The samples were thoroughly dried prior to the measurement.

were of lower density, modulus, and hardness than the corresponding composites formed with fillers made from micron-size quartz particles with polyurethanes. The SEM and SAXS of the nanocomposites showed that even at the highest loading, the filler particles failed to assume ordered packing. The progressive change in properties and increase in T_g with filler content occurred with both micron-size quartz and nanosilica, but more so with the latter, indicating that the filler particle affected the properties of the polyurethane matrix. There are two possible origins of such effect:

(1) chemical/physical interactions between the filler and the matrix,
(2) effects caused by geometrical constraints of the matrix resulting from the closed proximity of the filler particles.

Dielectric measurements showed that both the nonfilled sample and the filled composites exhibit an overlapping transition consisting of two subrelaxations, which become resolved at the highest frequencies only. The estimated activation energies of these transitions are around 200 and 100 kJ/mol, respectively, and the activation of the higher temperature transition is lower.

The polarization appearing above room temperature in most samples can probably be attributed to electrode polarization rather than to the MWS mechanism. It is possible, however, that in the nanosilica-filled sample stored under ambient conditions, a true MWS process appears at the wet filler–matrix interface.

The nanosilica exhibits stronger interaction with both the matrix polymer and water than the conventional filler, which can be explained by the higher specific surface area.

REFERENCES

1. Lipatov, Y. S. Fizicheskaya Khimiya Napolnenih Polimerov; Himiya: Moskva, 1977.
2. Lipatov, Y. S. Mezhfaznie Yavleniya v Polimerah; Naukova Dumka: Kiev, 1980.
3. Koberstein, J. T.; R. H., S. J Polym Sci: Polym Phys Ed 1983, 21, 1439.

4. Smith, T. L. J Polym Sci, Polym Phys Ed 1974, 12, 1825.
5. Chang, Y.-J.; Wilkes, G. L. J Polym Sci, Phys Ed 1975, 13, 455.
6. Petrović, Z. S.; Ferguson, J. Prog Polym Sci 1991, 16, 695.
7. Mark, J. E. Ceramic-Reinforced Polymers and Polymer-Modified Ceramics; ANTEC: Toronto, 1997; Vol. 2, p 1810.
8. Sun, C.-C.; Mark, J. E. Polymer 1989, 30, 104.
9. McCarthy, D. W.; Mark, J. E.; Schaefer, D. W.; J Polym Sci: Polym Phys 1998, 36, 1167.
10. McCarthy, D. W.; Mark, J. E.; Klarson, S. J.; Schaefer, D. W. J Polym Sci: Polym Phys 1998, 36, 1191.
11. Black, E. P.; Ulibarri, T. A.; Beaucage, G.; Schaefer, D. W.; Assink, R. A.; Bergstrom, D. F.; Giwa-Agbomeirele, P. A.; Burns, G. T.; ACS Polym Mater Sci Eng 1994, 70, 382.
12. Lu, S.; Melo, M. M.; Zhao, J.; Pearce, E. M.; Kwei, T. K. Macromolecules 1995, 28, 4908.
13. Goda, H.; Frank, C. W., ACS Polym Mater Sci Eng 1997, 77, 582.
14. Mark, J. E. Heterogeneous Chemistry Reviews 1996, 3, 307.
15. Siegel, R. W. ACS Polym Mater Sci Eng, 1995, 73, 26.
16. Guinier, A. Ann Phys 1939, 12, 161.
17. Porod, G. Koloid Z 1951, 124, 83.
18. Novak, B. M. Adv Mater 1993, 5, 422.
19. Kerner, E. H. Proc Roy Soc (B) 1956, 69, 808.
20. Nielsen, L. Mechanical Properties of Polymers and Composites; Marcel Dekker, Inc.: New York, 1974.
21. Wang, S. B.; Mark, J. E. Polymer Bulletin 1987, 17, 271.
22. McCrum, N. G.; Read, B. E.; Williams, G. Anelastic and Dielectric Effects in Polymeric Solids; Wiley: London and New York, 1967.
23. Hedvig, P. Dielectric Spectroscopy of Polymers; Akadémiai Kiadó: Budapest, 1977.
24. Dutta, J. Analusis Magazine 1996, 24, 16.
25. Ceramics and glasses; ASM International; 1991; Vol. 4.
26. Beek, L. K. H. v. Progress in Dielectrics; Heywood: London, 1967; Vol. 7.